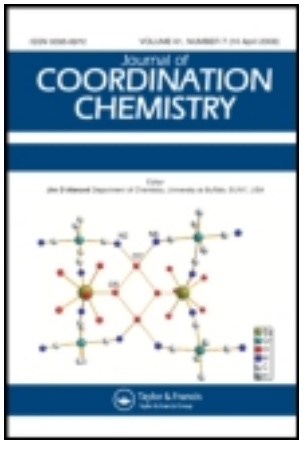

Journal of Coordination Chemistry
Publication details, including instructions for authors and subscription information:
http://www.tandfonline.com/loi/gcoo20

Synthesis, crystal structures, thermal, and spectroscopic properties of four new metal(II) (M=Co, Ni, Cu, Hg) complexes of 2-benzoylbenzoate with 3-picoline

Sema Caglar [a], Zerrin Heren [b] & Orhan Büyükgüngör [c]

[a] Department of Chemistry, Faculty of Arts and Sciences, Erzincan University, 24100, Erzincan, Turkey

[b] Department of Chemistry, Faculty of Arts and Sciences, Ondokuz Mayis University, 55200, Atakum, Samsun, Turkey

[c] Department of Physics, Faculty of Arts and Sciences, Ondokuz Mayis University, 55200, Atakum, Samsun, Turkey

Published online: 04 Aug 2011.

To cite this article: Sema Caglar, Zerrin Heren & Orhan Büyükgüngör (2011) Synthesis, crystal structures, thermal, and spectroscopic properties of four new metal(II) (M=Co, Ni, Cu, Hg) complexes of 2-benzoylbenzoate with 3-picoline, Journal of Coordination Chemistry, 64:15, 2706-2717, DOI: 10.1080/00958972.2011.605880

To link to this article: http://dx.doi.org/10.1080/00958972.2011.605880

Journal of Coordination Chemistry
Vol. 64, No. 15, 10 August 2011, 2706–2717

Synthesis, crystal structures, thermal, and spectroscopic properties of four new metal(II) (M = Co, Ni, Cu, Hg) complexes of 2-benzoylbenzoate with 3-picoline

SEMA CAGLAR*†, ZERRIN HEREN‡ and ORHAN BÜYÜKGÜNGÖR§

†Department of Chemistry, Faculty of Arts and Sciences, Erzincan University, 24100, Erzincan, Turkey
‡Department of Chemistry, Faculty of Arts and Sciences, Ondokuz Mayis University, 55200, Atakum, Samsun, Turkey
§Department of Physics, Faculty of Arts and Sciences, Ondokuz Mayis University, 55200, Atakum, Samsun, Turkey

(*Received 22 February 2011; in final form 13 June 2011*)

Four 2-benzoylbenzoate (bba) complexes, $[Co(bba)_2(H_2O)_2(3\text{-pic})_2]$ (**1**), $[Ni(bba)_2(H_2O)_2(3\text{-pic})_2]$ (**2**), $[Cu(bba)_2(3\text{-pic})_2]$ (**3**), and $[Hg(bba)_2(3\text{-pic})_2]$ (**4**), have been synthesized and characterized by IR spectra, thermal (TG, DTG, and DTA) analysis, and single crystal X-ray diffraction. All the complexes consist of neutral monomeric units with **1** and **2** crystallizing in the orthorhombic ($P\ n\ a\ 2_1$), **3** in triclinic ($P\bar{1}$), and **4** in monoclinic ($P2_1/c$) crystal systems. The metal(II) ions exhibit distorted octahedral coordination for **1**, **2**, and **3** and mercury(II) exhibits distorted trigonal prism coordination. In **1** and **2**, bba is monodentate, whereas in **3** and **4** bba is bidentate. 3-Picoline (3-pic) is a classical N-monodentate ligand. Bba are coordinated to metal(II) with carboxylates and IR spectra of all complexes display characteristic absorptions of carboxylate $\{\upsilon(OCO)_{asym}$ and $\upsilon(OCO)_{sym}\}$. Thermogravimetric (TG) analyses show that **1** and **2** are thermally stable ($T_{decomp.} > 60°C$) and **3** and **4** are thermally stable ($T_{decomp.} > 120°C$).

Keywords: 2-Benzoylbenzoic acid; 3-Picoline; Metal(II) complexes; Crystal structure

1. Introduction

Metal-carboxylate complexes have been recently used as metal organic framework materials with different structural features, physical, and chemical properties. They have a variety of applications, such as dyes, extractants, drugs, pesticides, catalysts, magnets, and host–guest chemistry [1–9].

Ligands containing carboxylates show different coordination modes, monodentate, chelate, and different types of bridges [10]; stable complexes of low coordination numbers could be available by flexible and sterically bulky ligands. 2-Benzoylbenzoic acid (Hbba) and its derivatives are used in the synthesis of supramolecular coordination compounds [11], in the preparation of electron-transport materials [11],

*Corresponding author. Email: semacaglar2002@hotmail.com

Journal of Coordination Chemistry
ISSN 0095-8972 print/ISSN 1029-0389 online
DOI: 10.1080/00958972.2011.605880

and sweeteners [12]. The crystal structure of 2-benzoylbenzoic acid (Hbba = $C_{14}H_{10}O_3$ and also named o-benzoylbenzoic acid) was investigated in 1990 [13], but studies of metal complexes of 2-benzoylbenzoate [bba = $(C_{14}H_9O_3)^-$] are few [11–20]. Bba is a polyfunctional ligand, due to the presence of the negatively charged carboxylate and carbonyl oxygens. 3-Picoline (3-pic) is used as a classical N-monodentate ligand to prepare mixed-ligand complexes.

This article reports the synthesis, spectral, thermal, and structural characterizations of four metal complexes of bba with 3-picoline.

2. Experimental

2.1. *Methods of sample characterization*

All reactions were performed with commercially available reagents without purification; solvents were distilled and dried by standard procedures. IR spectra were recorded on a Bruker Vertex 80V FT-IR spectrophotometer from 4000 to 450 cm^{-1} at a resolution of 4 cm^{-1} using KBr pellets. Electronic spectra were measured on a Unicam UV2 from 200 to 900 nm in methanol (MeOH). The C, H, and N contents of the complexes were determined with an Elementar Micro Vario CHNS. Room temperature magnetic susceptibility measurements were carried out using a Sherwood Scientific MXI model Evans magnetic balance. Thermal analysis curves (TG, DTA, DTG) were obtained simultaneously on a Perkin Elmer Diamond thermal analyzer in static air. A sample of 5–10 mg was used.

2.2. *Synthesis of [Co(bba)$_2$(H$_2$O)$_2$(3-pic)$_2$] (1)*

$Co(CH_3COO)_2 \cdot 4H_2O$ (0.075 g, 0.3 mmol) and 2-Hbba (2-benzoylbenzoic acid) (0.136 g, 0.6 mmol) were dissolved in MeOH–EtOH (mixture (1 : 1); 40 cm^3) with continuous stirring at reflux. Then 3-pic (98 μL, 1 mmol) was added dropwise to the solution. X-ray quality pink crystals of $[Co(bba)_2(H_2O)_2(3\text{-pic})_2]$ were obtained by slow evaporation of the solution at room temperature after 1 week. Yield: 70%. D.p.: 81°C. Anal. Calcd (%) for $C_{40}H_{36}N_2O_8Co$: C, 65.66; H, 4.92; N, 3.83. Found (%): C, 65.80; H, 4.65; N, 3.90.

2.3. *Synthesis of [Ni(bba)$_2$(H$_2$O)$_2$(3-pic)$_2$] (2)*

2-Hbba (0.136 g, 0.6 mmol) and $Ni(CH_3COO)_2 \cdot 4H_2O$ (0.075 g, 0.3 mmol) were dissolved in MeOH (40 cm^3) with continuous stirring at reflux. Then 3-pic (98 μL, 1 mmol) was added dropwise to the solution. Green crystals of $[Ni(bba)_2(H_2O)_2(3\text{-pic})_2]$ were obtained by slow evaporation at room temperature after 1 week. Yield: 70%. D.p.: 105°C. Anal. Calcd (%) for $C_{40}H_{36}N_2O_8Ni$: C, 65.68; H, 4.92; N, 3.83. Found (%): C, 65.80; H, 4.70; N, 3.91.

2.4. *Synthesis of [Cu(bba)$_2$(3-pic)$_2$] (3)*

2-Hbba (2-benzoylbenzoic acid) (0.136 g, 0.6 mmol) and $Cu(CH_3COO)_2 \cdot 2H_2O$ (0.06 g, 0.3 mmol) were dissolved in MeOH–EtOH (mixture (1 : 1); 40 cm^3) with continuous stirring at reflux. Then 3-pic (98 μL, 1 mmol) was added dropwise to the solution. X-ray quality blue crystals of $[Cu(bba)_2(3\text{-pic})_2]$ were obtained by slow evaporation of the solution at room temperature after day. Yield: 90%. D.p.: 160°C. Anal. Calcd (%) for $C_{40}H_{32}N_2O_6Cu$: C, 68.61; H, 4.57; N, 4.00. Found (%): C, 68.54; H, 4.70; N, 4.10.

2.5. *Synthesis of [Hg(bba)$_2$(3-pic)$_2$] (4)*

2-Hbba (0.136 g, 0.6 mmol) and $Hg(CH_3COO)_2 \cdot H_2O$ (0.098 g, 0.3 mmol) were dissolved in MeOH (40 cm^3) with continuous stirring at reflux. Then 3-pic (98 μL, 1 mmol) was added dropwise. Colorless crystals of $[Hg(bba)_2(3\text{-pic})_2]$ were obtained by slow evaporation at room temperature after 2 weeks. Yield: 76%. D.p.: 180°C. Anal. Calcd (%) for $C_{40}H_{32}N_2O_6Hg$: C, 57.40; H, 3.90; N, 3.30. Found (%): C, 57.20; H, 3.75; N, 3.15.

2.6. *X-ray crystallography*

Intensity data for **1**–**4** were collected using a STOE IPDS-II area detector diffractometer (MoKα radiation, $\lambda = 0.71073$ Å) at 293 K. The structures were solved by direct methods and refined on F^2 with SHELX-97 [21]. All non-hydrogen atoms were refined with anisotropic parameters. All hydrogens were included using a riding model. The details of data collection, refinement, and crystallographic data are summarized in table 1.

3. Results and discussion

3.1. *IR spectra*

Selected IR bands of Hbba and **1**–**4** are listed in table 2. The strong bands at 3649 cm^{-1} are due to υ(OH) of water ligands in **1** and **2**. Weak bands at 3050 and 2923 cm^{-1} are assigned to aromatic υ(CH) of phenyl rings and aliphatic υ(CH) of 3-pic, respectively, for **1**–**4**. Absorptions of the carbonyl of bba in the complexes are observed at 1668, 1669, 1670, and 1668 cm^{-1}, respectively. Carboxylate anions with typical $\upsilon(OCO)_{asym}$ values are 1546, 1546, 1561, and 1559 cm^{-1} and $\upsilon(OCO)_{sym}$ values are 1384, 1387, 1375, and 1381 cm^{-1}, respectively. The calculated $\Delta(OCO)$ $\{\upsilon(OCO)_{asym} - \upsilon(OCO)_{sym}\}$ of 162 cm^{-1} for **1** and 159 cm^{-1} for **2** are lower than the values expected for monodentate carboxylates (>200 cm^{-1}) but when such carboxylates are involved in hydrogen-bonding, reduction in the $\Delta(OCO)$ values is observed [22]. $\Delta(OCO)$ values $\{\upsilon(OCO)_{asym} - \upsilon(OCO)_{sym}\}$ of 186 cm^{-1} for **3** and 178 cm^{-1} for **4** are suitable for bidentate carboxylates (<200 cm^{-1}). Bands at 1581, 1566, and 1483 cm^{-1} correspond to υ(C=C) of bba and 3-pic; bands at 1275 cm^{-1} are due to υ(C–O). Medium intensity bands at 1604 cm^{-1} may be assigned for υ(C–N) of the aromatic ring of 3-pic,

Table 1. Crystal data and structure refinement parameters for **1**, **2**, **3**, and **4**.

	1	**2**	**3**	**4**
Empirical formula	$C_{40}H_{36}N_2O_8Co$	$C_{40}H_{36}N_2O_8Ni$	$C_{40}H_{32}N_2O_6Cu$	$C_{40}H_{32}N_2O_6Hg$
Formula weight	731.64	731.42	700.22	837.28
Temperature (K)	293	293	293	293
Wavelength (Å)	0.71073	0.71073	0.71073	0.71073
Crystal system	Orthorhombic	Orthorhombic	Triclinic	Monoclinic
Space group	*P n a* 2_1	*P n a* 2_1	$P\bar{1}$	$P2_1/c$
Unit cell dimensions (Å, °)				
a	18.5834(12)	18.7722(5)	7.7680(7)	14.7313(5)
b	9.5272(5)	9.4254(3)	8.7388(7)	15.3279(8)
c	20.4356	20.6322(5)	13.3609(12)	16.3478(6)
α	90	90	97.032(7)	90
β	90	90	99.032(7)	113.578(3)
γ	90	90	104.729(7)	90
Volume (Å)^3, *Z*	3618.1(3), 4	3650.57(18), 4	851.92(13), 1	3383.2(2), 4
Absorption coefficient (mm^{-1})	0.53	0.59	0.69	0.53
Calculated density (Mg m^{-3})	1.343	1.323	1.365	1.644
Crystal size (mm^3)	$0.09 \times 0.41 \times 0.62$	$0.54 \times 0.58 \times 0.64$	$0.23 \times 0.377 \times 0.58$	$0.16 \times 0.397 \times 0.56$
θ range for data collection (°)	2.0–26.5	1.97–26.35	2.5–27.1	1.5–26.5
Measured reflections	11,666	68,637	12,191	20,981
Independent reflections	6982	7360	3740	7021
Absorption correction[a]	Integration	Integration	Integration	Integration
Refinement method	Full-matrix least-squares on F^2	Full-matrix least-squares on F^2	Full-matrix least-squares on F^2	Full-matrix least-squares on F^2
Final *R* indices [$F^2 > 2\sigma(F^2)$]	0.1016	0.0640	0.0528	0.0530
Goodness-of-fit on F^2	0.845	1.074	1.039	0.911
Largest difference peak and hole (e Å^{-3})	−0.43 and 0.22	−0.420 and 1.384	−0.48 and 0.73	−0.70 and 0.55

[a]Ref. [23].

Table 2. Selected IR spectral data[a] for the Hbba ligand and **1–4**.

	Hbba	**1**	**2**	**3**	**4**
υ(OH)	3445m	3649s	3646s	–	–
υ_{aro}(CH)	3060w	3047w	3049w	3055w	3059w
υ_{alf}(CH)	–	2915w	2920w	2922w	2920w
υ(C=O)	1673vs	1668vs	1669vs	1670vs	1668vs
$\upsilon_{asym}(COO^-)$	–	1546m	1546m	1561m	1559s
$\upsilon_{sym}(COO^-)$	–	1384s	1387s	1375s	1381s
υ(C–O)	–	1274s	1274s	1278s	1277s
υ(C–N)	–	1604w	1604w	1607w	1602w

w, weak; m, medium; s, strong; vs, very strong.
[a]Frequencies in cm^{-1}.

confirming its presence in the adducts [24]. The bands under 600 cm^{-1} in **1–4** may be attributed to metal–oxygen and metal–nitrogen stretches.

3.2. *UV-Vis spectra and magnetic properties*

The electronic spectra of **1–4** are prepared in MeOH. Complex **1** exhibits mainly three maxima at 477 nm ($\varepsilon = 22$ $dm^3 mol^{-1} cm^{-1}$), 523 nm ($\varepsilon = 25\,dm^3 mol^{-1} cm^{-1}$), and

588 nm ($\varepsilon = 17\,dm^3\,mol^{-1}\,cm^{-1}$). Complex **2** shows only two bands with low intensity centered at 475 ($\varepsilon = 8\,dm^3\,mol^{-1}\,cm^{-1}$) and 607 nm ($\varepsilon = 9\,dm^3\,mol^{-1}\,cm^{-1}$) due to *d–d* transitions and a third band also appears at *ca.* 950 nm as evidenced from the shape of the spectra of the complex. Complex **3** has one absorption at 728 nm ($\varepsilon = 71\,dm^3\,mol^{-1}\,cm^{-1}$), assigned to *d–d* transitions. Complex **4** displays no transition above 400 nm. Intense bands at 220–300 nm are assigned to ligand-centered (*L–L**) transitions of bba and 3-pic.

The effective magnetic moments of **1**, **2**, and **3** at room temperature are 3.83, 2.74, and 1.52 B.M., respectively, consistent with the calculated values 3.87, 2.83, and 1.73 B.M., respectively.

3.3. *Thermal analysis*

Thermal behavior of **1** was followed to 900°C in static air. Complex **1** decomposes in three stages. The first between 60 and 109°C corresponds to the endothermic dehydration of the complex with a mass loss of 5.77% (Calcd mass loss 4.93%; $DTG_{max} = 81$°C). After dehydration, degradation of the two 3-pic and decomposition of the two bba occur in the second (109–306°C; $DTG_{max} = 280$°C) and third stage (306–438°C; $DTG_{max} = 361$°C) with a mass loss of 85.98% (Calcd mass loss 84.82%). The last mass loss step is vigorous and strongly exothermic (DTA at 391°C, 408°C) and related to the burning organic residue. Mass-loss calculations suggest that the product at 408°C is Co_3O_4, which further decomposes to CoO at 900°C.

Complex **2** also shows three stages of decomposition. In the first stage, endothermic dehydration occurs between 89 and 135°C with an experimental mass loss of 5.32% (Calcd mass loss 4.93%; $DTG_{max} = 105$°C). The second stage (135–301°C) is related to degradation of two 3-pic and one bba in an endothermic process (Found = 57.24, Calcd = 56.25%). The last stage (between 301 and 461°C) is extremely exothermic with bba abruptly burnt (DTA = 436°C). The total mass loss of all decomposition is 89.85% (Calcd 89.78%) and suggests that NiO is the end product.

Complex **3** shows two stages of decomposition. The first between 128 and 210°C corresponds to endothermic removal of one 3-pic with a mass loss of 13.12% (Calcd 13.29%). In the next stage, exothermic degradation of one 3-pic and two bba occurs at 210–505°C with a medium and one sharp exothermic DTA peaks at 248°C and 429°C, resulting in the formation of CuO. The experimental total mass loss value of 91.23% is consistent with the calculated value 89.63%.

Complex **4** begins to decompose with melting at 145°C and instantly decomposes after melting. The first stage between 120°C and 194°C corresponds to elimination of two 3-pic with a mass loss of 22.56% (Calcd 22.24%). Further decomposition occurs from 194 to 560°C with extremely exothermic DTA peaks at 497°C, 515°C and 545°C. Decomposition of the residue results in an empty crucible at *ca.* 580°C, suggesting that the final decomposition product is elemental mercury, which readily evaporates under these conditions.

3.4. *Description of the crystal structure of $[Co(bba)_2(H_2O)_2(3\text{-pic})_2]$ (1)*

Selected bond lengths and angles are given in table 3 and the hydrogen-bonding geometries are given in table 4. The complex crystallizes in the orthorhombic space

Table 3. Selected bond distances (Å) and angles (°) for **1**–**4**.

1			
Co1–N1	2.147(5)	O2–Co1–O5	179.58(19)
Co1–N2	2.145(5)	O2–Co1–O8	86.66(15)
Co1–O2	2.074(3)	O2–Co1–O7	91.24(15)
Co1–O5	2.074(4)	O5–Co1–O8	93.36(15)
Co1–O8	2.139(4)	O5–Co1–O7	88.73(17)
Co1–O7	2.150(4)	O5–Co1–N1	90.76(17)
O2–Co1–N1	89.66(18)	O5–Co1–N2	88.37(17)
O2–Co1–N2	91.21(17)	O8–Co1–N2	88.80(2)
O7–Co1–O8	177.86(19)	O8–Co1–N1	91.00(2)
O7–Co1–N2	90.83(17)	N2–Co1–N1	179.10(2)
O7–Co1–N1	89.40(2)		
2			
Ni1–N1	2.103(3)	O7–Ni1–O8	175.36(17)
Ni1–N2	2.101(4)	O7–Ni1–N2	90.21(16)
Ni1–O3	2.083(3)	O7–Ni1–N1	90.05(16)
Ni1–O6	2.087(3)	O6–Ni1–O8	89.48(15)
Ni1–O8	2.097(4)	O6–Ni1–O7	86.01(15)
Ni1–O7	2.112(4)	O6–Ni1–N1	92.17(14)
O3–Ni1–O6	178.72(15)	O6–Ni1–N2	89.59(14)
O3–Ni1–O8	91.78(16)	O8–Ni1–N2	88.67(17)
O3–Ni1–O7	92.72(15)	O8–Ni1–N1	91.21(17)
O3–Ni1–N1	88.01(15)	N2–Ni1–N1	178.24(18)
O3–Ni1–N2	90.24(14)		
3			
Cu1–N1	1.9991(19)	N1–Cu1–O1	89.29(7)
Cu1–O1	2.310(2)	N1–Cu1–O1^{i}	90.72(8)
Cu1–O2	2.108(2)	O2–Cu1–O2^{i}	180.00(5)
N1–Cu1–N1^{i}	180.00(5)	O2–Cu1–O1	59.02(7)
N1–Cu1–O2	89.89(8)	O2–Cu1–O1^{i}	120.98(7)
N1–Cu1–O2^{i}	90.11(9)	O1–Cu1–O1^{i}	180.00(1)
4			
Hg1–N1	2.374(3)	O5–Hg1–O2	116.73(11)
Hg1–N2	2.253(3)	O5–Hg1–O3	168.73(12)
Hg1–O2	2.316(3)	O5–Hg1–N1	87.25(11)
Hg1–O3	2.559(3)	O5–Hg1–O6	51.54(9)
Hg1–O5	2.255(3)	O2–Hg1–O3	53.43(9)
Hg1–O6	2.327(3)	O2–Hg1–N1	101.06(11)
N2–Hg1–O5	104.98(12)	O2–Hg1–O6	54.32(11)
N2–Hg1–O2	130.12(10)	O3–Hg1–N1	89.51(11)
N2–Hg1–N1	107.30(12)	O3–Hg1–O6	110.67(12)
N2–Hg1–O3	86.30(10)	O6–Hg1–N1	100.05(11)
N2–Hg1–O6	135.13(10)		

Symmetry code: (i) $-x, -y, -z$.

group $P\,n\,a\,2_1$. Each cobalt(II) is coordinated by two water molecules, two bba, and two 3-pic, forming an octahedral CoN_2O_4 coordination sphere. The two bba ligands are monodentate and 3-pic is also monodentate. $[Co(bba)_2(H_2O)_2(3\text{-pic})_2]$ is isostructural with $[Ni(bba)_2(H_2O)_2(3\text{-pic})_2]$. Their schemes are similar and shown in figure 1.

$Co–N_{3\text{-pic}}$ distance is 2.15(5) Å, which is slightly shorter than corresponding values in $[Co\{S_2P(OC_6H_4Me\text{-}p)_2\}_2(NC_5H_4Me\text{-}3)_2]$ (2.1755(3) Å) [24], $[Co\{S_2P(OC_6H_4Mep)_2\}_2(C_5H_5N)_2]$ (2.162(2) Å) [25], and $[Co\{S_2P(OEt)_2\}_2(C_5H_5N)_2]$ (2.164(3) Å) [26], where $S_2P(OC_6H_4Me\text{-}p)_2$, NC_5H_4Me-3 are bis(O,O°-ditolyl/dibenzyl/diphenyl dithiophosphato) and 3-picoline, but is significantly longer than 2.046(2) Å found in $[Co(3\text{-pic})_2Cl_2]$ [27].

Table 4. Hydrogen-bonding geometries for **1–3**.

D–H···A	D–H (Å)	H···A (Å)	D···A (Å)	D–H···A (°)
1				
O7–H7B···O3	0.813(19)	1.85(3)	2.618 (6)	158(7)
O8–H8B···O6	0.808(19)	1.83(2)	2.605 (6)	160(7)
2				
O7–H7A···O2	0.88(2)	1.83(3)	2.54(6)	135(7)
O8–H8A···O6	0.82(2)	1.77(2)	2.567(6)	163(7)
3				
C5–H5···O2	0.93	2.57	3.015(4)	109
C10–H10···O1	0.93	2.55	3.412(4)	154

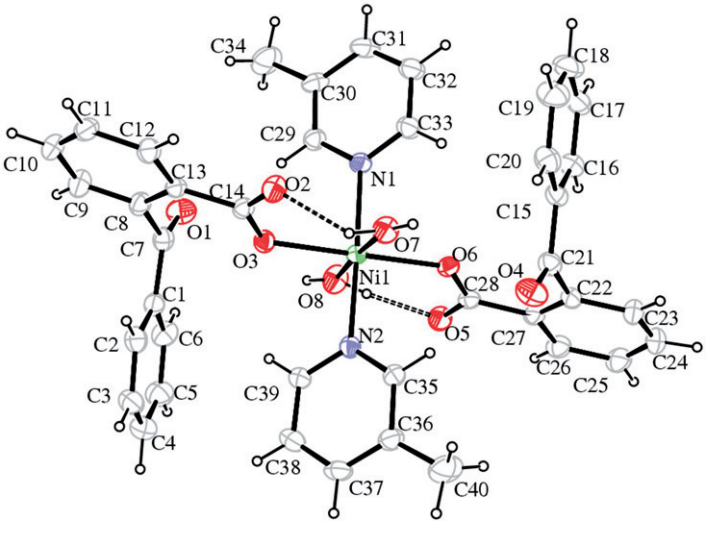

Figure 1. ORTEP III diagram and atom numbering of **2**. The hydrogen bond is drawn as dashed lines. Displacement ellipsoids are drawn at the 20% probability level (**1** is isostructural with **2**).

Co–O_{bba} bond distance of 2.074(3) Å is shorter than Co–$O4_{bba}$ (2.1366(18) Å) and $CoO5_{bba}$ (2.2238(17) Å) but bigger than Co–$O1_{bba}$ (2.0437(16) Å) in $[Co(bba)_2(H_2O)(phen)]$ [28].

There is an intramolecular hydrogen bond between the hydrogen of water and carboxylate oxygen of bba (table 4). There are C33–H33···Cg5 (2.73 Å) and C39–H39···Cg3 (2.76 Å) interactions between phenyl rings of bba and C–H of 3-pic.

3.5. *Description of the crystal structure of $[Ni(bba)_2(H_2O)_2(3\text{-pic})_2]$ (2)*

The crystal structure of **2** with atom numbering is shown in figure 1. Details of crystal data, data collection, structure solution, and refinement are given in table 1. Selected bond lengths and angles are given in table 3 and hydrogen-bonding geometries are given

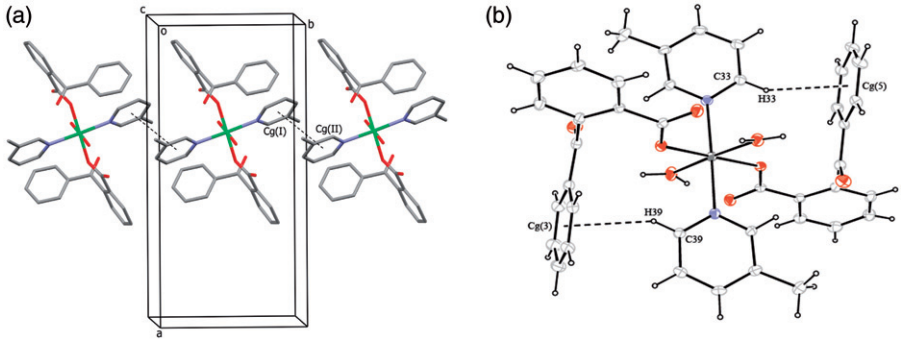

Figure 2. (a), (b) A crystal packing diagram of **2** showing $\pi\cdots\pi$ and C–H$\cdots\pi$ interactions.

in table 4. The structure of **2** is similar to **1**. Ni(II) is coordinated by two nitrogens from two 3-picoline and four oxygens from two 2-benzoylbenzoate and two water molecules in an octahedron (NiO_4N_2). The angles close to the ideal octahedral (180°) are O(3)–Ni(1)–O(6), N(2)–Ni(1)–N(1) and O(7)–Ni(1)–O(8) at 178.72(15), 178.24(18) and 175.36(17), respectively.

Ni–O_{bba} bond distances are 2.083(3) and 2.087(3) Å, which are slightly shorter than the corresponding value in $[Ni(bba)_2(et)_2(imidazole)_2]$ (2.094(3) Å) [19] and $[Ni(bba)_2(H_2O)(butOH)(phen)]$ (2.0996(14) Å) [28].

There are $\pi\cdots\pi$ interactions between pyridine rings of 3-pic [Cg1 = N1–C29–C30–C31–C32–C33 and Cg2 = N2–C35–C36–C37–C38–C39, Cg1–Cg2 = 4.02(3) Å for **2**]. There are also C33–H33$\cdots$Cg5 (C15, C16, C17, C18, C19, and C20) (2.73 Å) and C39–H39$\cdots$Cg3 (C1, C2, C3, C4, C5, and C6) (2.86 Å) interactions between phenyl rings of bba and C–H of 3-pic (figure 2).

There are intramolecular hydrogen bonds between hydrogen of water and carboxylate oxygen of bba (table 4) so that O7–H7A$\cdots$O2 and O8–H8A$\cdots$O6 intramolecular hydrogen bonds stabilize this arrangement.

3.6. *Description of the crystal structure of [Cu(bba)$_2$(3-pic)$_2$] (3)*

The crystal structure of **3** with atom numbering schemes is shown in figure 3. Details of crystal data, data collection, structure solution, and refinement are given in table 1. Selected bond lengths and angles are given in table 3 and hydrogen-bonding geometries are given in table 4. The structure of **3** is different from **1** and **2**. Water ligands are absent in **3**. Complex **3** consists of neutral molecules with copper(II) sitting on a centre of symmetry in distorted octahedral coordination made up of two bba which form the equatorial plane and two 3-pic occupying axial positions. Bba is bidentate and oxygen-coordinated.

Cu–$O(1)_{bba}$ bonds are longer than Cu–$O(2)_{bba}$ and Cu–$N(1)_{3\text{-pic}}$ bonds, resulting in formation of an elongated octahedron along the $O(1)_{bba}$ bonds, as a consequence of the Jahn–Teller effect.

Cu–O_{bba} distances are 2.107(2) and 2.311(2) Å, slightly longer than a corresponding value in $[Cu(bba)_2(benzimidazole)_2]$ (1.95(13) Å) [20]. Cu–$N_{3\text{-pic}}$ bond distance is

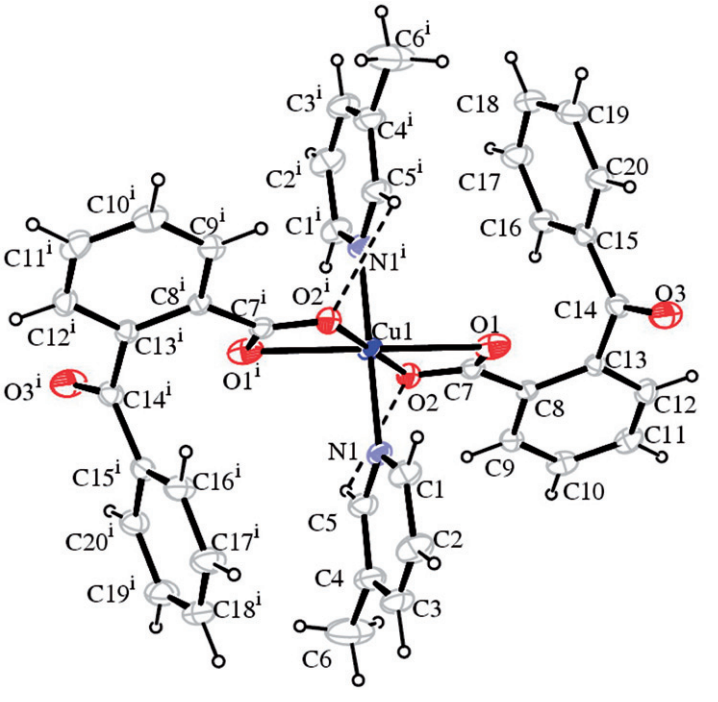

Figure 3. The molecular structure of **3** showing the atom-numbering scheme. Hydrogen bonds are drawn as dashed lines. Displacement ellipsoids are drawn at the 20% probability level.

1.999(2), similar to [*cis*-Cu(p-hydroxybenzoate)$_2$(3-picoline)$_2$] (1.99(2) Å) [29] and [Cu(2-Cl-5-FC$_7$H$_3$O$_2$)$_2$(3-pic)$_2$(H$_2$O)$_2$] (2.009(4) Å) [30] where 2-Cl-5-FC$_7$H$_3$O$_2$ is 2-chloro-5-fluorobenzoate.

There is an intramolecular hydrogen bond between hydrogen of carbon of 3-pic and carboxylate of bba (figure 4).

3.7. *Description of the crystal structure of [Hg(bba)$_2$(3-pic)$_2$] (4)*

A molecular view of **4** is shown in figure 5 and selected bond distances and angles are listed in table 3. The mercury(II) is a distorted trigonal prism with two 3-pic ligands and two bba ligands, forming a HgO_4N_2 coordination sphere. The two bba ligands are bidentate. The 3-pic is a monodentate nitrogen donor.

Hg–O_{bba} bond distances are 2.253(3) and 2.374(3) Å, similar to corresponding values in [Hg(sac)$_2$(py)$_2$] (2.26(5) and 2.32(5) Å) [31].

There is C5–H5 $\cdots$ Cg4 (C1, C2, C3, C4, C5, and C6) (2.65 Å) interaction between the phenyl rings of the bba ligands (figure 6).

4. Conclusion

Four new Co(II), Ni(II), Cu(II), and Hg(II) complexes containing bba and 3-pic, [Co(bba)$_2$(H$_2$O)$_2$(3-pic)$_2$], [Ni(bba)$_2$(H$_2$O)$_2$(3-pic)$_2$], [Cu(bba)$_2$(3-pic)$_2$], and

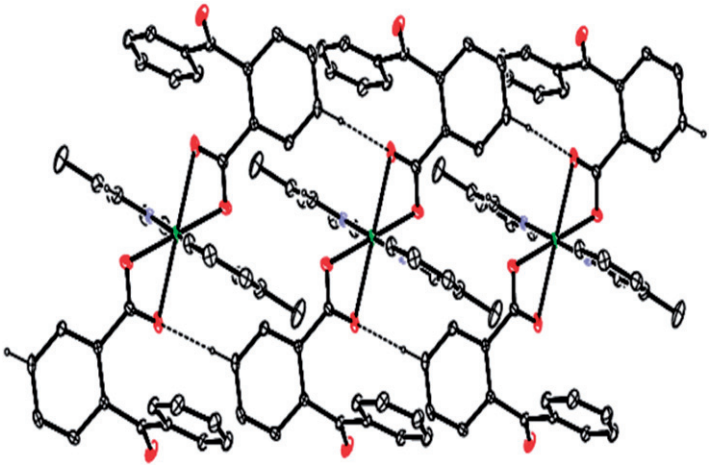

Figure 4. A crystal packing diagram of **3** showing hydrogen bonds.

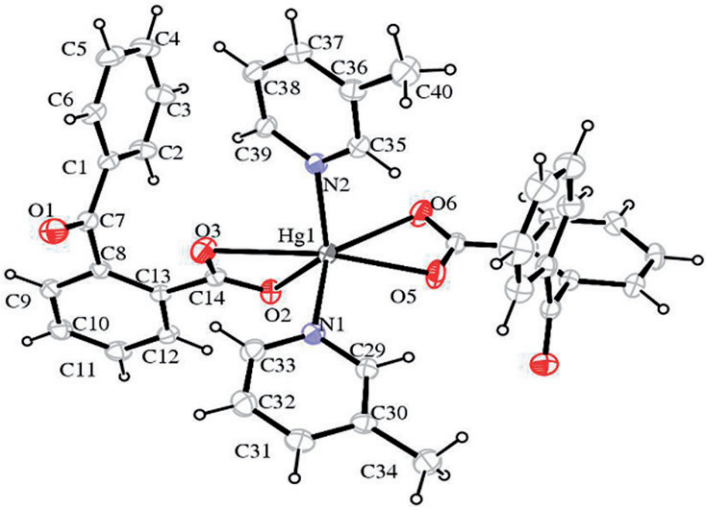

Figure 5. ORTEP III diagram and atom numbering scheme of **4**. Displacement ellipsoids are drawn at the 20% probability level.

$[Hg(bba)_2(3\text{-pic})_2]$, have been synthesized and characterized. All are mononuclear. **1** and **2** crystallize in the orthorhombic ($P\,n\,a\,2_1$), **3** in triclinic ($P\bar{1}$), and **4** in monoclinic ($P2_1/c$) crystal systems. The Co(II), Ni(II), and Cu(II) ions exhibit distorted octahedral coordination; Hg(II) exhibits distorted trigonal prism coordination. The crystal packing of the complexes are stabilized by C–H $\cdots\pi$ and $\pi\cdots\pi$ interactions between 3-pic and bba ligand. The room-temperature magnetic moment measurements show **1**, **2**, and **3** are paramagnetic; **4** is diamagnetic.

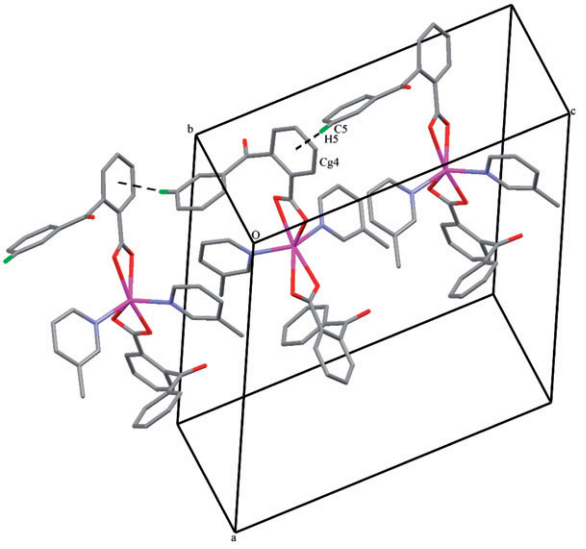

Figure 6. A crystal packing diagram of **4** showing C–H $\cdots\pi$ interactions.

Supplementary material

Crystallographic data for structural analysis have been deposited with the Cambridge Crystallographic Data Center, CCDC nos 812295 for **1**, 812294 for **2**, 812293 for **3** and 812296 for **4**. Copies of these information may be obtained free of charge from The Director, CCDC, 12 Union Road, Cambridge CB2 1 EZ, UK (Fax: +44 1223 336033; E-mail: deposit@ccdc.cam.ac.uk; www: http://www.ccdc.cam.ac.uk).

References

[1] C.N.R. Rao, S. Natarajan, R. Vaidhyanathan. *Angew. Chem., Int. Ed.*, **43**, 1466 (2004).
[2] Q. Chu, G.X. Liu, Y.Q. Huang, X.F. Wang, W.Y. Sun. *J. Chem. Soc., Dalton Trans.*, 4302 (2007).
[3] G. Blay, I. Fernandez, T. Gimenez, J.R. Pedro, R. Ruiz, E. Prdo, F. Lloret, M.C. Munoz. *Chem. Commun.*, **20**, 2102 (2001).
[4] P.G. Lassahn, V. Lozan, G.A. Timco, P. Christian, C. Janiak, R.E.P. Winpenny. *J. Catal.*, **222**, 260 (2004).
[5] R-H. Zhang, W.-S. Xia, H. Wang, Z.-H. Zhou. *Inorg. Chem. Commun.*, **12**, 583 (2009).
[6] M. Eddaoudi, D.B. Moler, H. Li, B. Chen, T.M. Reineke, M. O'Keeffe, O. Yaghi. *Acc. Chem. Res.*, **34**, 319 (2001).
[7] J. Moellmer, E.B. Celer, R. Luebke, A.J. Cairns, R. Staudt, M. Eddaoudi, M. Thommes. *Microporous Mesoporous Mater.*, **129**, 345 (2010).
[8] H. Li, M. Eddaoudi, M. O'Keeffe, O.M. Yaghi. *Nature*, **402**, 276 (1999).
[9] H. Furukawa, M.A. Miller, O.M. Yaghi. *J. Mater. Chem.*, **17**, 3197 (2007).
[10] R. Baggio, R. Calvo, M.T. Garland, O. Peña, M. Perec, L.D. Slep. *Inorg. Chem. Commun.*, **10**, 1249 (2007).
[11] D. Wang, H. Zhu, N. Shan, G. Song, J. Wang. *Acta Cryst.*, **E62**, 304 (2006).
[12] A. Arnoldi, A. Bassoli, G. Borgonovo, L. Merlini, G. Morini. *J Agric. Food Chem.*, **45**, 2047 (1997).
[13] R.A. Lalencette, P.A. Vanderhoff, H.W. Thompson. *Acta Cryst.*, **C46**, 1682 (1990).
[14] M.R.J. Foreman, M.J. Plater, J.M.S. Skakle. *J. Chem. Soc., Dalton Trans.*, 1897 (2001).
[15] Y. Song, B. Yan, Z. Chen. *J. Coord. Chem.*, **58**, 1417 (2005).

[16] C.A.K. Diop, A. Toure, L. Diop, R. Welter. *Acta Cryst*., **E62**, m3338 (2006).
[17] L. Liu, Z. Xu, Z. Lou, F. Zhang, B. Sun, J. Pei. *J. Rare Earths*, **24**, 253 (2006).
[18] L. Liu, Z. Xu, Z. Lou, F. Zhang, B. Sun, J. Pei. *J. Lumin*., **122–123**, 961 (2007).
[19] Z. Heren, H. Paşaoğlu, M.H. Yıldırım, D. Hıra. *Acta Cryst*., **E65**, 907 (2009).
[20] M.H. Yıldırım, Z. Heren, H. Paşaoğlu, D. Hıra, O. Büyükgüngör. *Acta Cryst*., **E65**, 638 (2009).
[21] G.M. Sheldrick. *Acta Cryst*., **A64**, 112 (2008).
[22] M. Devereux, M. McCann, V. Leon, R. Kelly, D. O'Shea, V. McKee. *Polyhedron*, **22**, 3187 (2003).
[23] Stoe & Cie. *X-AREA (version 1.18) and X-RED32 (version 1.04)*. Stoe & Cie, Darmstadt, Germany (2002).
[24] S. Bajia, A. Mishra, R.J. Butcher, K.G. Ojha. *J. Coord. Chem*., **63**, 4271 (2010).
[25] S.C. Bajia, J.E. Drake, M.E. Light, M. Nirwan, S.K. Pandey, R. Ratnani. *Polyhedron*, **28**, 85 (2009).
[26] Z. Xhu, J.H. Lin, Y.P. Yu, J. Xu, X.Z. You, S.X. Liu, C.C. Lin. *Huaxue Xuebao*, **7**, 623 (1989).
[27] D. Wyrzykowski, E. Styezen, Z. Wranke. *Transition Met. Chem*., **31**, 860 (2006).
[28] S. Caglar, Z. Heren, O. Büyükgüngör. *J. Coord. Chem*., **64**, 1289 (2011).
[29] R.P. Sharma, A. Singh, A. Saini, P. Venugopalan, A. Molinari. *J. Mol. Struct*., **888**, 291 (2009).
[30] R.P. Sharma, A. Saini, S. Singh, A. Singh, P. Venugoplan, P. Starynowicz, J. Jezierska. *J. Mol. Struct*., **988**, 9 (2011).
[31] Z.S. Seddigi, A. Banu, G.M. Golzar Hossain. *Arab. J. Sci. Eng*., **32**, 181 (2007).